

Shallow water agglutinated foraminiferal response to Late Cretaceous–Early Paleocene sea-level changes in the Dakhla Oasis, Western Desert, Egypt

Sreepat Jain ^{a,*}, Sherif Farouk ^b

^a Department of Geology, School of Applied Natural Science, Adama Science and Technology University, 1888 Adama, Oromia, Ethiopia

^b Exploration Department, Egyptian Petroleum Research Institute, Nasr City, 11727, Egypt



ARTICLE INFO

Article history:

Received 17 March 2017

Received in revised form

8 June 2017

Accepted in revised form 15 June 2017

Available online 21 June 2017

Keywords:

Late Cretaceous

Paleocene

Agglutinated foraminifera

Shallow water

Egypt

ABSTRACT

The Late Cretaceous (Maastrichtian) to early Paleocene (Thanetian) shallow water (<100 m) agglutinated foraminifera from a section at Dakhla Oasis (Western Desert, Egypt) were analyzed for their assemblage, species and genera distribution, diversity, depositional environment, community structure and palaeobathymetry with respect to regional tectonics, climate and global eustasy. Data suggest an equitable benthic environment with low species dominance deposited in a brackish littoral and/or marsh setting. Sea level curves using characteristic benthic foraminiferal species, genera and assemblages corroborate quantitatively generated estimate and statistical analysis. Data suggests that in the absence of or of an impoverished benthic foraminiferal fauna, a high resolution agglutinated foraminiferal dataset can be as good a predictor of the benthic community structure and environment, as its calcareous counterpart, at least for shallow settings (<100 m). Present data also provides a good window in better understanding the distribution and interrelationship between the three dominant genera, *Haplophragmoides*, *Trochammina* and *Ammobaculites*. Faunal changes at boundaries (Cretaceous/Paleogene, Danian/Selandian and Selandian/Thanetian) are also evaluated.

© 2017 Elsevier Ltd. All rights reserved.

1. Introduction

The Late Cretaceous–Paleocene agglutinated benthic foraminifera have been used as an effective proxy for inferring changes in palaeobathymetry, palaeoenvironment, paleoxygenation and palaeoproductivity both at the basinal level (deep-sea environment; Kaminski 2008; Kaminski and Geroch, 1992; Kuhnt et al., 1996; Kuhnt and Urquhart, 2001; Galeotti et al., 2004; Setoyama et al., 2011; Kochhann et al., 2014) and for shallow settings (Petters, 1979; Kaminski, 1987; Luger, 1988a; Gebhardt, 1998; Nagy et al., 2000, 2013; Kaminski et al., 2008, 2010; Farouk and Jain, 2016); the former studies abound whereas those for the latter, are rare.

Recently, the benthic foraminiferal diversity and assemblages of the shallow water Maastrichtian–Danian (in part) interval (samples 1–247) from the Dakhla Oasis (Egypt) were studied to infer changes in palaeobathymetry, palaeoenvironment,

palaeoproductivity and sea-level by Farouk and Jain (2016), identifying thirteen foraminiferal assemblages; the emphasis was on calcareous benthic foraminifera. The present study uses the same framework of assemblages and extends both the assemblages (14–19) and sampled duration from Danian to Thanetian (sample 237–315) and accesses the entire dataset (315 samples) with the sole emphasis of using the abundance distribution of agglutinated foraminifera to access species and genera distribution, diversity, depositional environment, community structure and palaeobathymetry with respect to regional tectonics, climate and global eustasy. The agglutinated foraminifera constitute 0–90% of the benthic foraminiferal assemblage (see Table 1).

Thus, the rationale for doing this contribution is to document (a) the distributional pattern of agglutinated foraminifera in a shallow water setting, (b) the usefulness of agglutinated foraminifera as an effective independent and robust proxy for safely accessing the prevailing depositional environment, species diversity and community structure, palaeobathymetry, and changes in sea-level, (c) that the benthic foraminiferal-based sea level curve successfully replicates the transfer function-based estimate, (d) to test the hypothesis that if analyzed independently, the agglutinated

* Corresponding author.

E-mail address: sreepatjain@gmail.com (S. Jain).

foraminifera are as good a proxy for faithfully reflecting the prevailing benthic community structure and environment as their calcareous counterpart, at least for shallow settings (<100 m), and (c) above all, to increase the meager (global and regional) body of work on shallow water agglutinated foraminifera.

The present contribution, also provides a high-resolution (315 samples) window for better understanding the distribution and interrelationship between the three dominant shallow water-setting genera of *Haplophragmoides*, *Trochammina* and *Ammobaculites* for the Maastrichtian–Thanetian interval in Egypt.

2. Geological setting

Records of Late Cretaceous (Maastrichtian) to Paleocene (Thanetian) agglutinated foraminifera from Egypt are very scarce and those that are there, are largely taxonomic in nature (Abd El Hameed, 1973; Faris, 1974; Lüger, 1988b; Orabi, 1995, 2000; Hewaidy et al., 2014). The Dakhla Oasis (Western Desert) provides good exposures (Fig. 1) for studying benthic foraminifers (both calcareous: see Hewaidy et al., 2006; Farouk and Jain, 2016; and agglutinated, this study). It is also the biggest oasis in the Western Desert of Egypt, and lies between longitudes 28°15'–29°40' E and latitudes 25°00'–26°00' N (Fig. 1). Lithologically, the Dakhla Oasis comprises a very thick and well-exposed Upper Cretaceous (Maastrichtian) to Paleocene (Thanetian) succession characterized by lateral and vertical facies variations represented by two facies types, Garra El-Arbain, and Nile Valley (see Fig. 1); the present paper deals with the latter (for details see Issawi, 1972; El-Azabi and Farouk, 2011; El Nady and Hammad, 2015; Farouk, 2016).

2.1. Lithostratigraphy

The studied Quart El Mawohb section (Fig. 1) is divided into two Formations, the basal Dakhla Shale and upper Tarawan Chalk (see Fig. 2).

2.1.1. Dakhla Shale Formation

The Dakhla Shales, an informal term used to describe the shales and mudstones overlying the Duwi Formation and underlying the Tarawan Chalk Formation (Said, 1962; Awad and Ghobrial, 1965) constitutes the Dakhla Formation which is further subdivided into three formal Members, Mawhoob Shale, Beris Oyster Mudstone and Kharga Shale, from base upwards (see Fig. 2).

2.1.1.1. Mawhoob Shale member. These are the basal laminated black shales interbedded with siltstones that overly the Duwi Formation and underlie the Beris Oyster Mudstone Member (samples 1–77; see Fig. 2). The shale is calcareous, fissile, gray to black, and silty.

2.1.1.2. Beris Oyster mudstone member. The member consists of gray to reddish gray shales intercalated with argillaceous limestones, sandstones, and siltstones (samples 78–148; see Fig. 2); the Member is marked by the abundance of the bivalve, *Exogyra overwegi* von Buch.

2.1.1.3. Kharga Shale member. This is divided into two units, namely Lower (samples 149–200; see Fig. 2) and Upper (samples 201–305; see Fig. 3). The Kharga Shale Member consists of pale to dark gray and green calcareous, partly glauconitic, and phosphatic shales intercalated with siltstones, sandstones, and limestones. In the middle, a 20–30 cm thick phosphatic conglomeratic band, represents an erosional disconformity – a hiatus, the Cretaceous/Tertiary boundary (K–Pg, henceforth; between samples 200–201).

Table 1
Agglutinated foraminiferal assemblage discussed in the text. The basic framework on which they are based is given in the first column (19 calcareous benthic foraminiferal assemblages of Farouk and Jain, 2016).

Benthic assembly	Sample numbers	% Agglutinated	% average	HOFs	Most abundant species	Genera	Agglutinated Bioclasts	Proposed paleodepth
19	306–315	2.87	28.70	9.10	<i>Spiroplectinella esauensis</i>	<i>Haplophragmoides excavata</i>	<i>Spiroplectinella</i>	Outer neritic to upper bathyal
18	289–305	21.38	9.10	6.60	No agglutinated foraminifera (dominated by calcareous Epistomina and Cibicides)No agglutinated foraminifera (dominated by calcareous Epistomina and Cibicides)	<i>Haplophragmoides gibra</i>	<i>Haplophragmoides</i>	Littoral to inner neritic
17	285–288	0.00	0.00					
16	282–284	66.67	0.00		<i>Haplophragmoides excavata</i>	<i>Haplophragmoides</i>		
15	267–281	40.48	9.60		<i>Haplophragmoides gibra</i>	<i>Ammobaculites subcretaceous</i>	<i>Ammobaculites</i>	
14	255–266	38.61	6.90		<i>Haplophragmoides excavata</i>	<i>Haplophragmoides glabra</i>	<i>Haplophragmoides</i>	
13	239–254	28.81	16.60		<i>Haplophragmoides excavata</i>	<i>Ammobaculites subcretaceous</i>	<i>Ammobaculites</i>	
12	217–238	90.63	0.00		<i>Haplophragmoides gibra</i>	<i>Trochammina juncea</i>	<i>Trochammina</i>	
11	202–216	31.62	7.60		<i>Haplophragmoides excavata</i>	<i>Trochammina simplex</i>	<i>Trochammina</i>	
10	191–201	13.51	17.80		<i>Trochammina rainwateri</i>	<i>Trochammina digonis</i>	<i>Trochammina</i>	
9	165–190	10.65	0.00		<i>Trochammina rainwateri</i>	<i>Trochammina digonis</i>	<i>Trochammina</i>	
8	149–164	19.10	14.50		<i>Trochammina雨wateri</i>	<i>Trochammina雨wateri</i>	<i>Trochammina雨wateri</i>	
7	128–148	9.70	14.00		<i>Haplophragmoides calcula</i>	<i>Ammobaculites</i>	<i>Ammobaculites</i>	
6	100–127	49.41	42.90		<i>Haplophragmoides calcula</i>	<i>Haplophragmoides calcula</i>	<i>Haplophragmoides calcula</i>	
5	86–99	9.92	20.40		<i>Haplophragmoides hindsii</i>	<i>Ammobaculites</i>	<i>Ammobaculites</i>	
4	74–85	68.99	0.00		<i>Haplophragmoides hindsii</i>	<i>Trochammina rainwateri</i>	<i>Trochammina rainwateri</i>	
3	46–73	60.03	1.40		<i>Ammobaculites khargensis</i>	<i>Trochammina rainwateri</i>	<i>Trochammina rainwateri</i>	
2	18–45	40.63	0.00		<i>Ammobaculites khargensis</i>	<i>Ammobaculites</i>	<i>Ammobaculites</i>	
1	1–17	20.34	7.30		<i>Ammomarginulina austerae</i>	<i>Cribrostomoides trinitensis</i>	<i>Ammomarginulina</i>	Upper bathyal

HOFs: High organic-flux species.

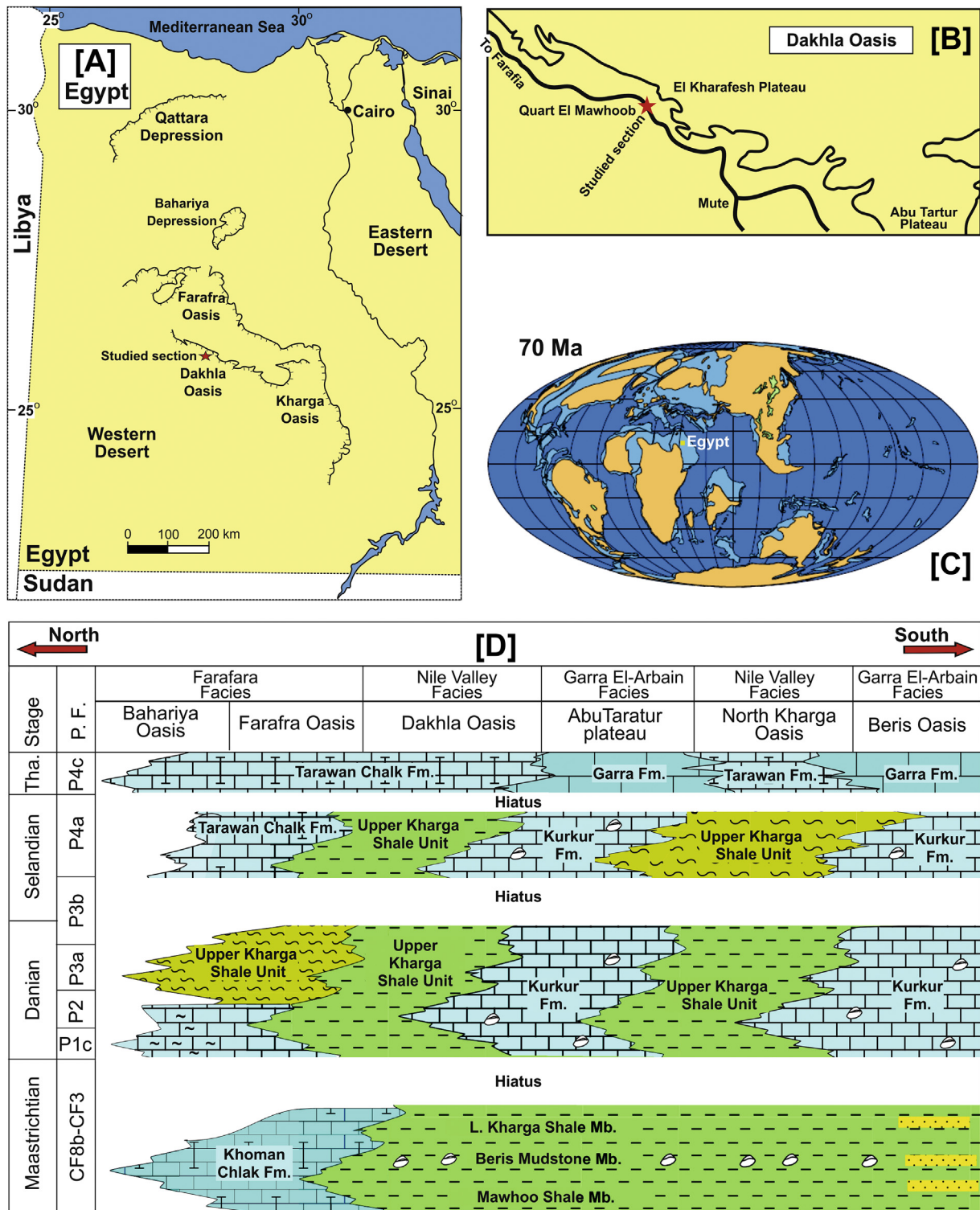


Fig. 1. (A) Locality map of Egypt. The star in the center marks the location of the studied section; (B) expanded view of the studied section; (C) the paleogeographic map during the Cretaceous; (D) regional lithostratigraphy showing the extent of the Maastrichtian–Thanetian sediments exposed at the Dakhla Oasis.

2.1.2. Tarawan Chalk Formation

The predominantly snow-white chalky limestones that unconformably overlie the Dakhla Shale Formation constitute the Tarawan Chalk Formation (samples 306–315; see Fig. 2). The unconformity is marked by an irregular surface with bioturbated marl to silty

clays with limestone nodules, and a ferruginous sandstone at the top. In detail, these limestones are made up of white, snow-white to yellowish white, hard, thickly bedded chalk and chalky limestone with few marl and shale intercalations. These limestones form top scarp faces of the eastern plateaus surrounding the Dakhla Oasis.

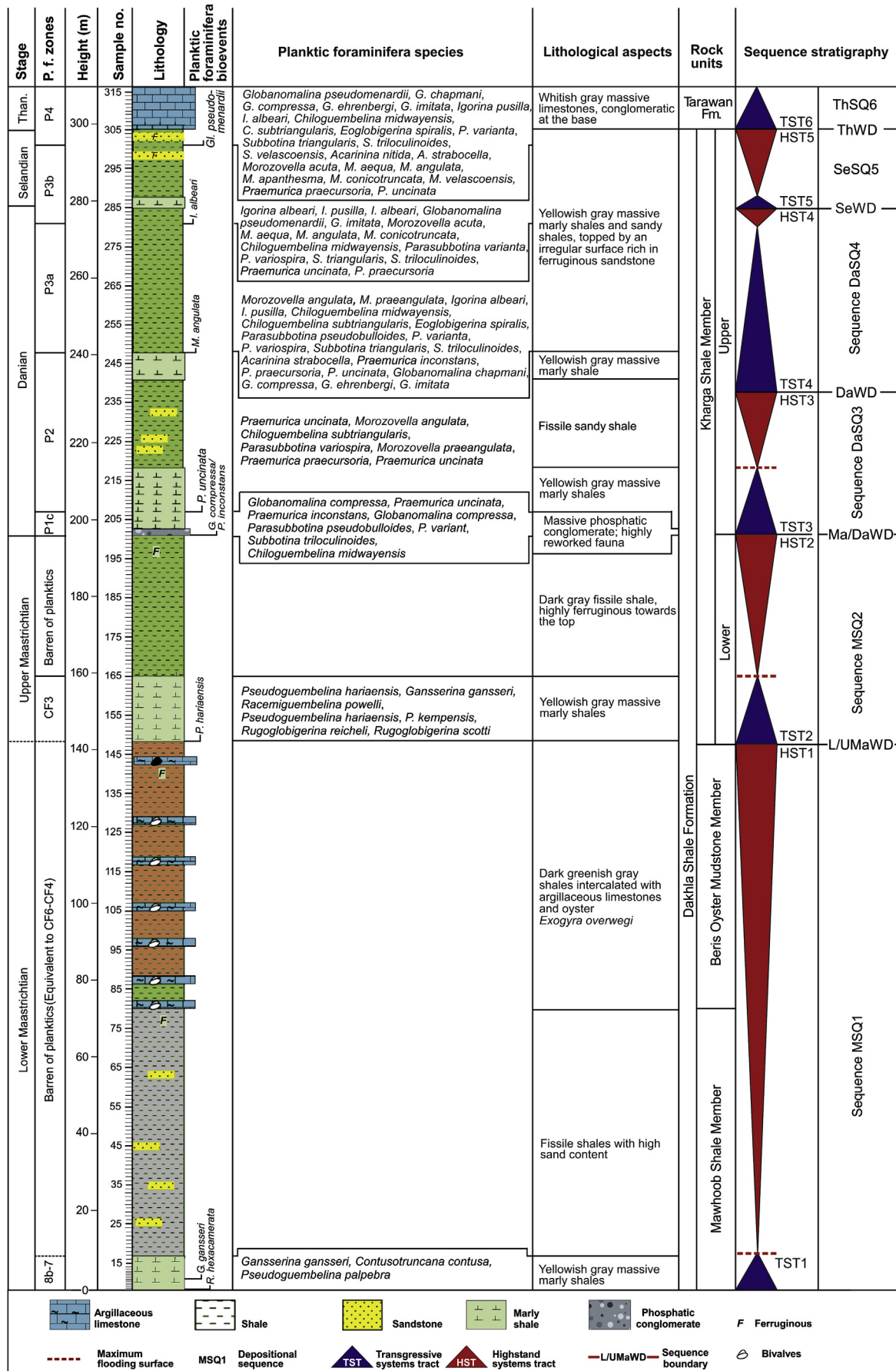


Fig. 2. Lithostratigraphy, biostratigraphy (planktic foraminifera) and sequence stratigraphy of the studied rock.

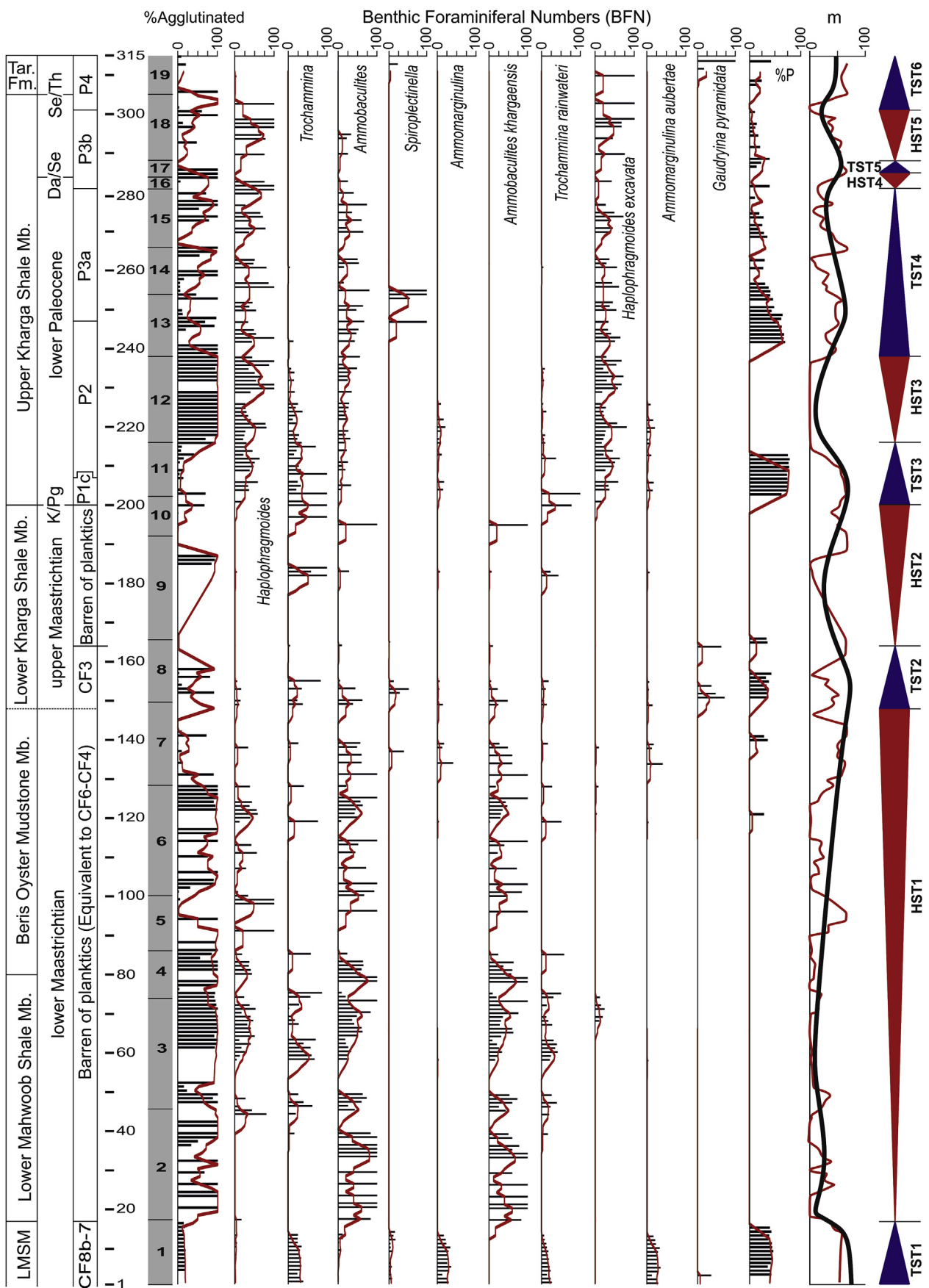


Fig. 3. The distribution of dominant agglutinated genera and species, benthic foraminiferal assemblages (marked by the gray block with numbers from 1 to 19), % Planktic, qualitatively inferred sea level and TR sequences identified in the present work. All dark lines (red) are 5-point running averages. (For interpretation of the references to color in this figure legend, the reader is referred to the web version of this article.)

2.2. Biostratigraphy

The studied rocks range in age from Maastrichtian (CF7) to Thanetian (P4) (Fig. 2). The planktonic foraminiferal zonal schemes followed here are after Li et al. (1999) and Huber et al. (2008) for the Maastrichtian and that of Keller et al. (1995), Keller et al. (2002), Berggren and Pearson (2005) and Wade et al. (2011) for the Paleocene.

The Maastrichtian records three Zones, CF8b, CF7 and CF3 based on the first appearance of *Rugoglobigerina hexacamerata* Brönnemann, *Gansserina gansseri* (Bolli) and *Pseudoguembelina hariaensis* Nederbragt, respectively; separated by a non-diagnostic/barren interval (see Fig. 2). It is interesting to note that the FAD (First Appearance Datum) of *G. gansseri*, in GSSP and standard zonations, appears at the uppermost Campanian (see Huber et al., 2008), but in the Middle East, it appears within the lower Maastrichtian (see Farouk, 2014).

The Paleocene has six Zones, P1c, P2, P3a, P3b and P4. The FO (First Occurrence) of the *Globanomalina compressa* and/or *Paramurica varianta* (P1c) is recorded at the base of the Kurkur Formation (not studied here but see Hewaidy et al., 2006). The lower boundary of the P1d Zone is marked by the FO of *Praemurica trinidadensis*, noted at the base of the upper Kharga Shale unit (see Fig. 4). P1d/P2 and P2/P3a zonal boundaries are marked by the FO of *Praemurica uncinata* and *Morozovella angulata*, respectively. These zones are recorded within the upper Kharga Shale unit (see Fig. 2). The P3a/P3b zonal boundary is marked by the FO of the *Igorina albeari*. The FO of the *Globanomalina pseudomenardii* marking the base of the P4 Zone is recorded within the uppermost part of the Dakhla Formation (see Fig. 2). Berggren and Pearson (2005) subdivided P4 Zone into three subzones, but in the present study, poor preservation and rarity of the planktonic foraminifera within this interval makes it difficult to follow this subdivision. Details for each planktonic foraminiferal zones is summarized in Appendix 1.

3. Boundaries

3.1. The Cretaceous/Paleogene boundary (K/Pg)

The K/Pg boundary (between samples 200–201) separates the lower and upper units of the Kharga Shale Member and is marked by absence of the latest Maastrichtian planktic Zones CF2 and CF1 and the presence of the earliest Paleocene P1a, and P1b Zones (see Fig. 2). The base of Paleocene in the Dakhla Oasis is characterized by the Bir Abu Munqar Horizon (see Barthel and Herrmann-Degen, 1981; Farouk, 2016). It consists of ~30 cm to 1 m layer of phosphatic conglomeratic marl rich in reworked and in situ Danian foraminifera.

3.2. The Danian/Selandian boundary (Da/Se)

Obaidalla et al. (2009) delineated the Da/Se boundary at the base of the 25 cm thick organic-rich phosphatic shale layer within the upper part of the Dakhla Formation that lies at the boundary between *Igorina albeari*/*Praemurica carinata* and *Igorina albeari* planktic Zones (Fig. 2). The boundary is characterized by a short-term sea-level fall coinciding with the P3a–P3b boundary (see also Speijer, 2003; Obaidalla et al., 2009). Farouk and El-Sorogy (2015) placed the Da/Se boundary within the *Igorina albeari* (P3b) subzone and stated that in the Central and Southern Western Desert, the boundary is represented by an unconformity marked by the absence of the topmost part of the *Igorina albeari*/*Globanomalina pseudomenardii* (P3b) subzone. In the present study, the Da/Se boundary is placed within the *Igorina albeari* Zone (between samples 284–285; see Fig. 2).

3.3. Selandian/Thanetian boundary (Se/Th)

A hiatus near the base of the Thanetian stage is recorded in most part of Egypt and is characterized by a condensed interval and a facies change from the calcareous shales of the Dakhla Shale Formation to the limestones of the Tarawan Chalk Formation (see also Faris and Farouk, 2012; Farouk, 2016). In the present study, a 10 cm thick, gravelly mudstone bed with an irregular basal surface marks the boundary between the two formations (between samples 304–305; Fig. 2).

4. Sequence stratigraphy

Six third order sequence boundaries are identified that characterize sedimentation and faunal breaks (erosional, lack of biozones, reworking, facies shifts, and sharp changes in biofacies) (see Fig. 2). These are named using an abbreviation of their assigned stage boundaries coupled with an abbreviation of the term Western Desert (L/UMaWD, Ma/DaWD, DaWD, SeWD and ThWD; see Fig. 2). The inferred sequence boundaries record the presence of three third-order depositional sequences which are named using the first letter of the assigned stage followed by an abbreviation of the term sequence with a running number counted separately for each stage (MSQ1, MSQ2, DaSQ1, etc.). The sequences represent a transgressive-regressive system tracts (TST–HST), where the lowstand systems tract (LST) are rarely initiated due to the deposition in an intra-shelf basin characterized by the presence of submerged palaeo-structural highs and lows (see also El-Azabi and Farouk, 2011; Farouk and Jain, 2016). The identified sequences are summarized in Appendix 2 and include: Sequence MSQ1 (TST1 and HST1), Sequence MSQ2 (TST2 and HST2), Sequence DaSQ3 (TST3 and HST3), Sequence DaSQ4 (TST4), Sequence DaSQ5 (TST5 and HST5) and Sequence DaSQ6 (TST6) (see Fig. 2).

5. Methods

The present study deals with the distribution of Maastrichtian–Thanetian shallow water agglutinated foraminifers that make up 0–90% of the total benthic foraminiferal assemblage (see Table 1). A total of 190 samples (of the studied 315) have yielded 4118 agglutinated foraminifera specimens (see Table 2). The 125–63 µm fraction from 2 g of sediments was investigated qualitatively and quantitatively under the binocular zoom stereomicroscope. The agglutinated foraminiferal dataset (4118 specimens) is analyzed for its temporal species and genera distribution (Fig. 3), diversity (Fig. 4–5), depositional environment and community structure (Fig. 6), and palaeobathymetry (Fig. 7). Additionally both agglutinated and calcareous benthic foraminiferal dataset are also analyzed separately for diversity and (Fig. 8) and community structure (Fig. 9) for the studied duration to independently evaluate their reflection of the prevailing environment. A summary of all proxies is given in Fig. 10. Both sea level curves are further accessed in light of the revised Cretaceous eustasy (Haq, 2014) (Fig. 11).

Among the above-mentioned proxies, the Benthic Foraminifera Number (BFN; the number of specimens per gram) is used infer subtle changes in oxygenation and organic matter flux (Fig. 3). This, when inferred in conjunction with the dominant agglutinated genera (*Trochammina*, *Haplophragmoides* and *Ammobaculites*) and species (*Ammobaculites khargaensis*, *Haplophragmoides excavata*, *Trochammina rainwateri*, *Ammomarginulina aubertae* and *Gaudryina pyramidata*) (see Fig. 3) provide a robust estimate of the prevailing palaeoenvironment. Among the Diversity measures [Shannon–Weaver information function (Shannon H), Fisher's alpha (α), Equitability (E) and Dominance (D)] and Species abundance are used (Figs. 4–5). Diversity measures (Shannon H, Fisher's α ,

Equitability and Dominance) are further used to provide a better estimation of the prevailing ecological structure and depositional environment (Fig. 6).

Paleobathymetry (relative sea level) is inferred by using the presence of characteristic agglutinated and benthic species, the abundance values of calcareous benthic foraminifers and the presence and abundance of planktic foraminifers (%P; see Fig. 3). The following gradational approach with respect to %P is followed: 1–5% P, 10–50 m, inner neritic; 8–25% P, 50–100, middle neritic; 25–75% P, 100–200 m, outer neritic, and 78–90% P, 200–600 m, upper bathyal (see also Olsson and Nyong, 1984; Koutsoukos and Hart, 1990; Hewaidy et al., 2014). The %P does not exceed 80% in the present study (see Fig. 3).

Additionally, paleobathymetry is also calculated following the transfer function given by Van der Zwaan et al. (1999) and compared with the qualitative benthic foraminiferal estimate (see Fig. 7). Van der Zwaan et al. determined a regression for the relationship between bathymetry and the percentage of planktonic foraminifera (%P), based on present-day bathymetric transects (Equation 1)

$$\text{Depth (in m)} = e^{3.58718 + (0.03534 * \%P)} \quad (1)$$

where %P = percentage planktics in the total foraminiferal association, is calculated as $100 * P / (P + B)$, P = number of planktic specimens and B = number of benthic specimens. The deep infaunal species (i.e. dwelling well below the sediment–water interface; = the high organic-flux species of present work; HOFS; see Fig. 4) and therefore not directly dependent on the flux of organic matter to the sea floor, forms the basis for the depth relation of regression (Equation 1) are not used in the calculations as several of these taxa are seen to dominate benthic assemblages under unfavorable circumstances and are then commonly indicated as stress-markers (see also Van der Zwaan et al., 1999; van Hinsbergen et al., 2005). These are omitted from the determination of %P. The planktic fraction %P is then calculated as: %P = $100 * (P / (P + B))$ where S = number of stress markers (deep infaunal = High organic-flux species of present work; HOFS; see Fig. 4). The omitted HOFS species include *Anomalinoides aegyptiacus*, *Bolivina cretosa*, *Bolivina decurrans*, *Bulimina prolixa*, *Bulimina strobili*, *Neobulimina canadensis*, *Neobulimina khagaensis*, *Nonionella africana*, *Nonionella insecta*, *Praebulimina carseyae*, *Praebulimina kikapoensis*, *Praebulimina russi*, *Pyramidulina affinis*, *Pyramidulina distans*, *Pyramidulina semispinosa*, *Pyramidulina vertebralis*, *Pyramidulina zippei* and *Reussella aegyptiaca*.

Additionally, statistical analysis is also carried out to access the interrelationship of the dominant agglutinated foraminiferal genera (Appendix 3), species diversity (Appendix 4), the interrelationship between benthic foraminiferal inferred bathymetry, transfer function-based calculated bathymetry, and planktic, benthic and total BFN (Benthic Foraminifera Numbers) numbers (see Appendices 5–6), relationship of the dominant genera, *Trochammina* with %P and Calcareous BFN (Appendix 7) and the comparison of agglutinated and calcareous benthic foraminiferal diversity proxies (Appendix 8).

6. Results

This contribution bears out 4 fundamental results:

1. Five agglutinated foraminiferal biofacies are identified (that encompass 19 calcareous benthic foraminiferal assemblages); the former display depth-dependence (see Table 1).
2. The distribution pattern of these agglutinated biofacies also faithfully reflect changes in paleoenvironment, paleoxxygenation, paleoproductivity and community structure.

3. Three (Dominance, Evenness and Equitability) of the five (Fisher's α and Shannon H; positive but not significant) agglutinated and calcareous foraminiferal diversity proxies are positively and significantly correlated to each other (see Figs. 8–9; Appendix 8).

4. The results from this contribution demonstrate that a high resolution agglutinated foraminiferal dataset can be as effective a tool for inferring benthic community structure and environment as their calcareous counterpart (see Figs. 8–9; Appendix 8).

6.1. Paleobathymetry

Qualitative paleobathymetry based on the presence of characteristic species, the abundance values of calcareous benthic foraminifers and the presence and abundance of planktonic foraminifers suggests a largely shallow neritic shelf environment (<100 m) for the entire studied section (see Fig. 7).

Quantitative paleobathymetry calculated by using the transfer function of Van der Zwaan et al. (1999) parallels the qualitative-based sea level curve; both are also statistically significant (Appendix 6a) and largely remain within the 100 m paleodepth (see Fig. 7). However, the transfer function based calculation of the sea level is much higher at two places (and incidentally also coincides with the intervals of maximum values of %P, i.e. during Zones P1c and at the transition between P2 and P3a) (see Fig. 7). When these two anomalously high values are removed and the statistical correlation done, the significance is maintained and the Pearson Correlation value improves considerably (from 0.028 to 0.58; see Appendix 6b; N = 315 and 294, respectively).

6.2. Genera and species distribution (Assemblage)

Unlike the previously studied calcareous benthic foraminifera (Farouk and Jain, 2016), the agglutinated ones do not display any preference for a particular T–R sequence (see Fig. 3). However, when considered as a group (biofacies) (see Table 1), and based on the framework of 19 benthic foraminiferal assemblages, they seem to follow a well-constrained pattern (see Table 1). *Ammobaculites*, *Haplophragmoides* and *Trochammina* (make up 78% of the total agglutinated population; see Table 2) follow the sea level curve (see Fig. 3); the shallow infaunal coarsely agglutinated *Ammobaculites* dominates in the pre-K–Pg stable, but largely shallow neritic environment (see Table 1 and Fig. 3), *Haplophragmoides*, another shallow infaunal coarsely agglutinated form, does so in the post-K–Pg slightly deeper but fluctuating environment; and lastly, the epifaunal *Trochammina* dominates in the intervening times of maximum sea level rise and higher %P (see Table 1 and Fig. 5). Also, respectively, at the corresponding species level, *Ammobaculites khargaensis*, *Haplophragmoides excavata* and *Trochammina rainwateri* dominate (see Table 1 and Fig. 3). *Ammomarginulina aubertae* dominates in the upper Campanian CF7 planktic foraminiferal Zone at the base of the section, whereas *Gaudryina pyramidata* does so in the lower part of the upper Maastrichtian CF3 Zone (see Fig. 3).

Additionally, it is interesting to note that a positive and statistically significant relationship is noted between paleodepth and the agglutinated genera *Gaudryina*, *Ammomarginulina*, *Spiroplectinella* and *Cribrostomoides* (see Appendix 3). Interestingly, studies show that these four have a preference for outer neritic–upper bathyal depths. *Trochammina* also shows positive correlation with paleodepth but not significantly (see Appendix 3). On the other hand, both *Haplophragmoides* (statistically significant) and *Ammobaculites* (though not significant) show negative correlation with paleodepth (see Appendix 3). *Haplophragmoides*, the dominant agglutinated genus, interestingly shows positive and statistically

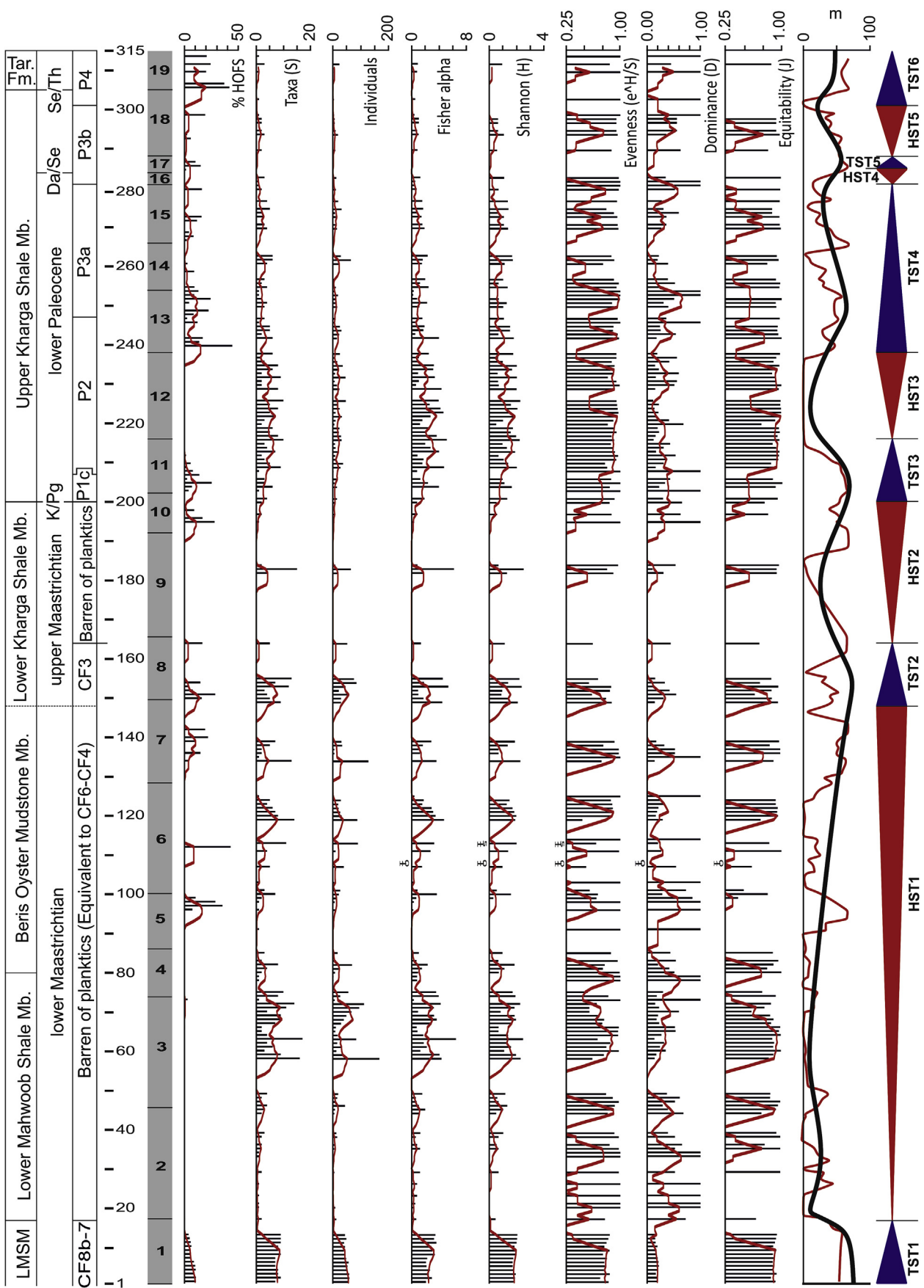


Fig. 4. Benthic foraminiferal diversity, benthic foraminiferal assemblages (marked by the gray block with numbers from 1 to 19), qualitatively inferred sea level and TR sequences identified in the present work. All dark lines (red) are 5-point running averages. (For interpretation of the references to color in this figure legend, the reader is referred to the web version of this article.)

significant correlation with both *Trochammina* and *Ammobaculites* (see Appendix 3). Numerous studies have demonstrated that all three (*Haplophragmoides*, *Trochammina* and *Ammobaculites*) proliferate at shallow depths (littoral to inner neritic) (see Berggren, 1974a,b; Lüger, 1985; Speijer, 1994; Sprong et al., 2012).

Agglutinated species- and genera-wise, five biofacies are recognized that reflect not only the prevailing paleoenvironment but also the paleodepth (see Table 1; Fig. 3). Biofacies 1 is represented by *Ammomarginulina* (*A. aubertae*), 2 by *Ammobaculites* (*A. khargaensis*), 3 by *Trochammina* (*T. rainwateri*), 4 by *Haplophragmoides* (*H. excavata*) and 5 by *Spiroplectinella* (*S. esnaensis*) (see Table 1; Figs. 3 and 10). Biofacies 5 is marked by an unusual increased presence of high organic-flux species and a sudden increase in %P (see Figs. 3 and 10).

6.3. Diversity

The relationship between the two main diversity indices – Fisher's α and Shannon H is positive and statistically significant (0.900; significant at the 0.01 level; 2-tailed) suggesting that both are good proxies for representing diversity. Hence, Fisher's α is used here as a diversity representative.

The Calcareous BFN that positively and significantly correlates with % P represents deeper paleodepths (see Appendix 4). The Agglutinated BFN (proxy for shallower depths) correlates positively and significantly with Fisher's α , number of Taxa, number of Individuals and Equitability and negatively and significantly with Dominance and Evenness (see Appendix 4).

On an average diversity values decrease from the base of the studied section in the lower Maastrichtian (CF7; TST1) to the top, in the Thanetian (P4 Zone; TST6) (see Fig. 7). The diversity values are highest at TST1 followed by an abrupt decline in the succeeding HST1 and then a gradual increase until HST3 which records another high, and then a rapid decline until the end of the section in TST6 (see Fig. 5). Like the agglutinated species and genera, there seems to be no clear correlation between diversity values and TR cycles (TST/HST), however, diversity values are higher during TST (see Fig. 5). The most remarkable aspect of the present dataset is the high values of species Evenness and Equitability and low values for Dominance (see Fig. 4).

6.4. Depositional environment and community structure

The plot of Fisher's α versus Shannon H gives a robust estimate of the depositional environment and the prevailing foraminiferal community structure (see Fig. 6). All data points, except 4 that plot in the open marine shelf environment, plot in the restricted brackish lagoonal/marsh region (see Fig. 6).

6.5. Sea level curve

The sea level curve based on qualitative and quantitative estimates (as explained above) is not only positively correlated but is also statistically significant (Appendices 5–6). Both suggest a largely shallow neritic environment (<100 m paleodepth; see Fig. 7). Broadly, high sea level persisted during late Campanian time, followed by a sudden shallowing and then a gradual increase throughout the early Maastrichtian (see Fig. 7). A sea level rise during planktic foraminiferal CF3 Zone, was quickly followed by a shallowing just before the K–Pg boundary. Thereafter, sea level rise is noted during K–Pg and the P1c Zone with a decrease in the middle of the succeeding P2 Zone. The transition between P2 and P3a Zones records another sea level rise followed by decreases during transitions between Zones P3a–P3b and P3b–P4. This is followed by increases during Zones P3b and P4.

Table 2
Basic data discussed in the text.

Study material	Number of specimens		
Calcareous specimens	12,778		
Agglutinated specimens	4118		
Total specimens	16,896		
% Calcareous	75.6		
% Agglutinated	24.4		
Top 9 genera (= 95.3%)	Number of specimens	In percentage	
Genus			
<i>Ammobaculites</i>	1171	28.4	78.0
<i>Trochammina</i>	1032	25.1	
<i>Haplophragmoides</i>	1011	24.6	
<i>Ammomarginulina</i>	218	5.3	
<i>Gaudryina</i>	189	4.6	
<i>Spiroplectinella</i>	138	3.4	
<i>Reophax</i>	85	2.1	
<i>Bathysiphon</i>	57	1.4	
<i>Cribrostomoides</i>	24	0.6	
Top 9 species (67.3%)	Number of specimens	Percentage	
<i>Ammobaculites khargaensis</i>	672	17.4	40.9
<i>Trochammina rainwateri</i>	481	12.5	
<i>Haplophragmoides excavata</i>	425	11.0	
<i>Ammomarginulina aubertae</i>	218	5.7	
<i>Gaudryina pyramidata</i>	189	4.9	
<i>Haplophragmoides calcula</i>	168	4.4	
<i>Ammobaculites subcretaceous</i>	156	4.0	
<i>Trochammina umiatensis</i>	147	3.8	
<i>Haplophragmoides glabra</i>	139	3.6	

6.6. Comparative diversity, depositional environment and community structure

To discern the extent of how well the agglutinated foraminifera are able to faithfully reflect the prevailing benthic environment and community structure, independent of their calcareous counterpart, the diversity proxies are plotted next to each other (Figs. 8–9). Both follow similar trends (Figs. 8–9). Three (Dominance, Evenness and Equitability) of the five (Fisher's α and Shannon H; positive but not significant) agglutinated and calcareous foraminiferal diversity proxies are positively and significantly correlated to each other (Appendix 8). The former three proxy values (Dominance, Evenness and Equitability) for agglutinated dataset are somewhat consistently higher and lower for the latter two (Fisher's α and Shannon H; see Fig. 8). The only noticeable variance between the diversity proxies of agglutinated and calcareous foraminifera are for Assemblages 3, 4 and 12, all marked by very low % high organic-flux species (HOFS) (see Table 1; Fig. 3). However, when plotted against each other, they have similar trends and equally high R^2 values (see Fig. 9).

A summary (trends) of all results is given in Fig. 10 along with benthic foraminiferal assemblages.

7. Discussion

This contribution bears out 5 fundamental points:

1. The old fashioned judicious use of characteristic benthic foraminiferal species, genera and assemblages to infer paleobathymetry corroborates quantitative estimates (based on transfer functions and statistics). An integrated approach of using several old fashioned proxies (inference from assemblages, presence of characteristic species, the abundance values of calcareous benthic foraminifers and the presence and abundance of planktonic foraminifers), can produce robust inferences.

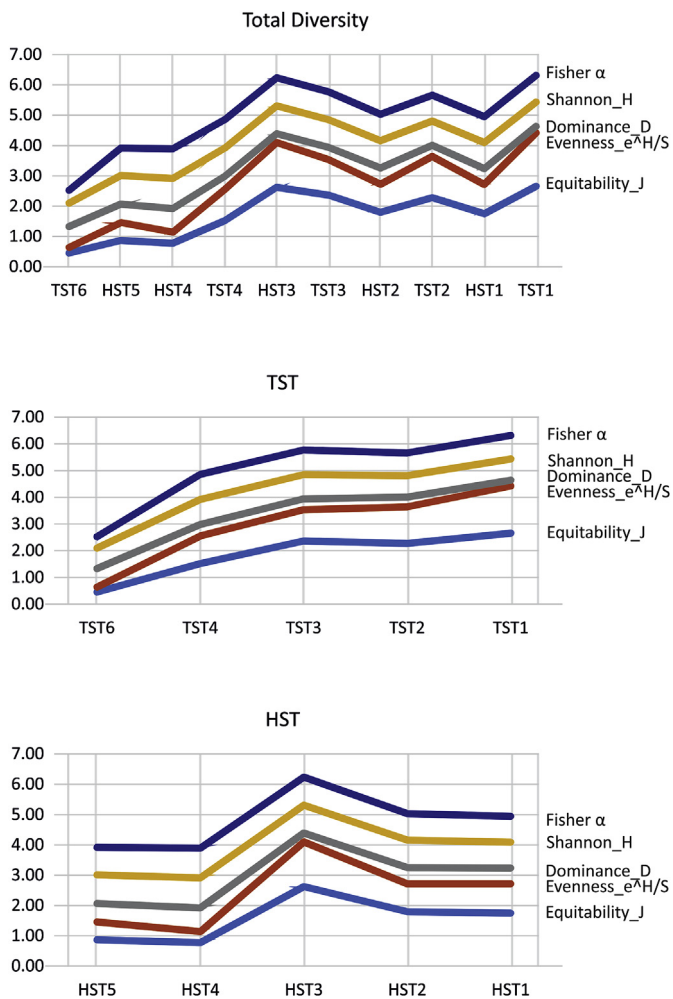


Fig. 5. Diversity plotted against TR sequences across the studied section.

2. The fact that three (Dominance, Evenness and Equitability) of the five (Fisher's α and Shannon H; positive but not significant) agglutinated and calcareous foraminiferal diversity proxies are positively and significantly correlated to each other (see Appendix 8), and that the plot of agglutinated and calcareous Fisher's α and Shannon H have the same trend (with equally high R^2 values; 0.901 and 0.896, respectively) suggests that the agglutinated benthic foraminiferal dataset reflects equally well (and with close accuracy), the prevailing benthic community structure and environment. This result suggests that in absence of benthic foraminifera, a high resolution agglutinated foraminiferal dataset can be as good a predictor of the benthic community structure, as its calcareous counterpart, at least for shallow settings, as this one (<100 m).
3. Based on agglutinated foraminiferal dataset, a largely equitable benthic environment with low dominance of species is noted, deposited in a brackish littoral and/or marsh setting.
4. Qualitative inferences from the abundance pattern of agglutinated species, genera and assemblages are well corroborated by robust statistical analysis.
5. This study provides a good window in better understanding the distribution and interrelationship between the most common neritic genera, *Haplophragmoides*, *Trochammina* and *Ammobaculites*.

The fact that both qualitative and quantitative estimates for approximating sea level rise and fall, are positively and significantly

correlated, indicates that the traditional species interpretation still holds good to the rigors of statistical analysis (Fig. 7). The only place where these two estimates (qualitative and quantitative) do not match are at TST3 and TST4 that incidentally also registers maximum % P (65–70 and 75–80, respectively), signifying considerable deepening, at least to upper bathyal depths (see Figs. 7 and 10). Interestingly, both TST cycles are dominated by the coarsely agglutinated *Haplophragmoides excavata* (within the agglutinated population; see Figs. 3 and 10), and calcareous benthic foraminiferal species *Anomalinoides zitllie* (TST3) and *Cibicidoides howelli* (TST4); all post-K–Pg (see Figs. 3 and 10). TST3, which covers the lower part of the planktic foraminiferal zone P1c, in fact represents a global sea level high (see Fig. 11) and TST4 which covers zone P3a, also records a regionally increasing sea level (see also Tantawy et al., 2001; Keller et al., 2002). Both *A. zitllie* and *C. howelli* are characteristic outer neritic–upper bathyal forms, whereas *Haplophragmoides excavata*, a littoral to outer neritic form. It is likely that aided by regional tectonics (regionally, P1c was an interval of increased subsidence; see Tantawy et al., 2001) and coupled with increased sea level, new niches opened leading to higher abundances. Interestingly, in these two intervals of anomalously high values, the small, low oxygen-tolerant planktic foraminifera, heterohelicids, also show peak abundances (see also Keller et al., 2002) as also increased levels of benthic higher organic flux species (HOFS; see Figs. 7 and 10). However, data from other sections, might shed more light on these anomalies. Overall, the inferred sea level curve matches well with the revised Cretaceous eustasy of Haq (2014) (see Fig. 11).

Statistical analysis bears out interesting interrelationship between the three dominant genera – *Haplophragmoides*, *Trochammina* and *Ammobaculites*. Both *Haplophragmoides* and *Ammobaculites* show a preference for shallower depths, however, *Trochammina* prefers deeper settings (Appendix 7 and Fig. 3). The distribution of other dominant agglutinated genera *Gaudryina*, *Ammomarginulina*, *Spiroplectinella* and *Cribrostomoides* are in expected lines, positively and significant correlated with paleodepth (see Appendix 3). All four are also characteristic outer neritic–upper bathyal genera.

Another important statistical outcome is about diversity indices. Data corroborates the long understood phenomenon that diversity increases in shallower depths; all diversity indices (except Dominance and Evenness) are positively and significantly correlated with Agglutinated BFN, considered here as a proxy for shallower depths as 78% of it is made up of *Haplophragmoides*, *Trochammina* and *Ammobaculites* (see Appendix 4; Table 2). In an equitable environment, as this one, Dominance (and of species and number of specimens, taxa and individuals, respectively) would understandably be low (negative) (see also Fig. 8).

As regards the community structure and the prevailing depositional environment, the plot of Shannon H versus Fisher's α mirrors the abundance pattern of the three dominant genera *Haplophragmoides*, *Trochammina* and *Ammobaculites*, also suggesting a largely restricted brackish lagoonal/marsh environment (Fig. 12). Only 4 data points plots outside in the open marine shelf region (see Fig. 6).

The comparison of species diversity between the agglutinated and calcareous foraminiferal dataset (Figs. 8–9) suggests that in the absence of or in case of an impoverished benthic foraminiferal dataset, a high resolution agglutinated foraminiferal dataset can be as good a predictor of the benthic community structure and environment, as its calcareous counterpart, at least for shallow settings (<100 m) (see Figs. 8–9). The only variance between the diversity proxies are noted for Assemblages 3, 4 and 12, all marked by very low % high organic-flux species (HOFS) and shallow depths (see Table 1; Fig. 8) suggesting that an agglutinated foraminiferal dataset of depths between 25 and 100 m may well serve to

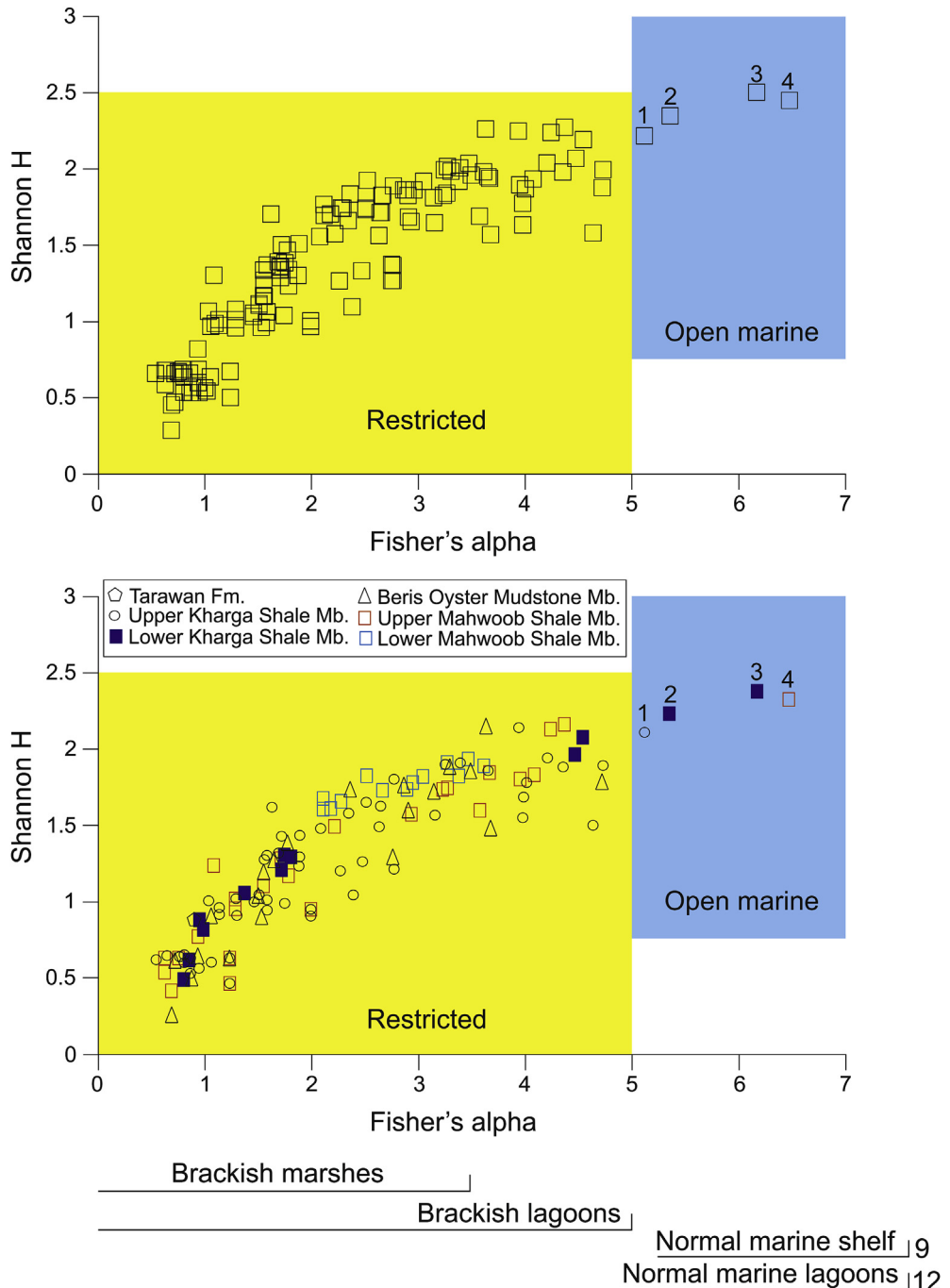


Fig. 6. Community structure and depositional environment of the studied section. Only four square agglutinated data points plot in the open marine region. They are: 1: sample 216 (TST3); 2: sample 153 (TST2); 3: sample 183 (HST2); 4: sample 63 (HST1). Samples 1, 2 and 3 belong to the deeper water agglutinated biofacies 3 (*Trochammina*) and sample 4 to the shallower biofacies 3 (see also Table 1).

compliment the same inference that are arrived at from a calcareous benthic foraminiferal dataset.

As regards boundary conditions, the change before and after K-Pg is most dramatic; the fauna changes from a *Trochammina*-dominated to a *Haplophragmoides*-dominated environment, from an epifaunal to a shallow infaunal habitat, from eutrophic to a mesotrophic environment, suggesting an increased role of organic flux (see Figs. 3 and 10). Species diversity registers a marked change to higher value (see Figs. 4–5 and 8). The species Dominance remains low and both Evenness and Equitability remain high, throughout the studied section arguing for an equitable

environment in a stable bottom environment (see Figs. 4–5 and 8). The Danian–Selandian boundary that straddles the benthic foraminiferal assemblages 16 and 17 also registers a dramatic change marked by the total absence of agglutinated foraminifera in the Selandian assemblage 17 (see Fig. 10 and Table 1). The Selandian–Thanetian boundary, between benthic foraminiferal assemblages 18 and 19, also records a marked change in both fauna and paleodepth, from a *Haplophragmoides* (*H. excavata*–*Haplophragmoides glabra*) dominated assemblage to that of a *Spiroplectinella* (*Spiroplectinella esnaensis*–*H. excavata*); the latter, a characteristic outer neritic–upper bathyal genera (see also Table 1).

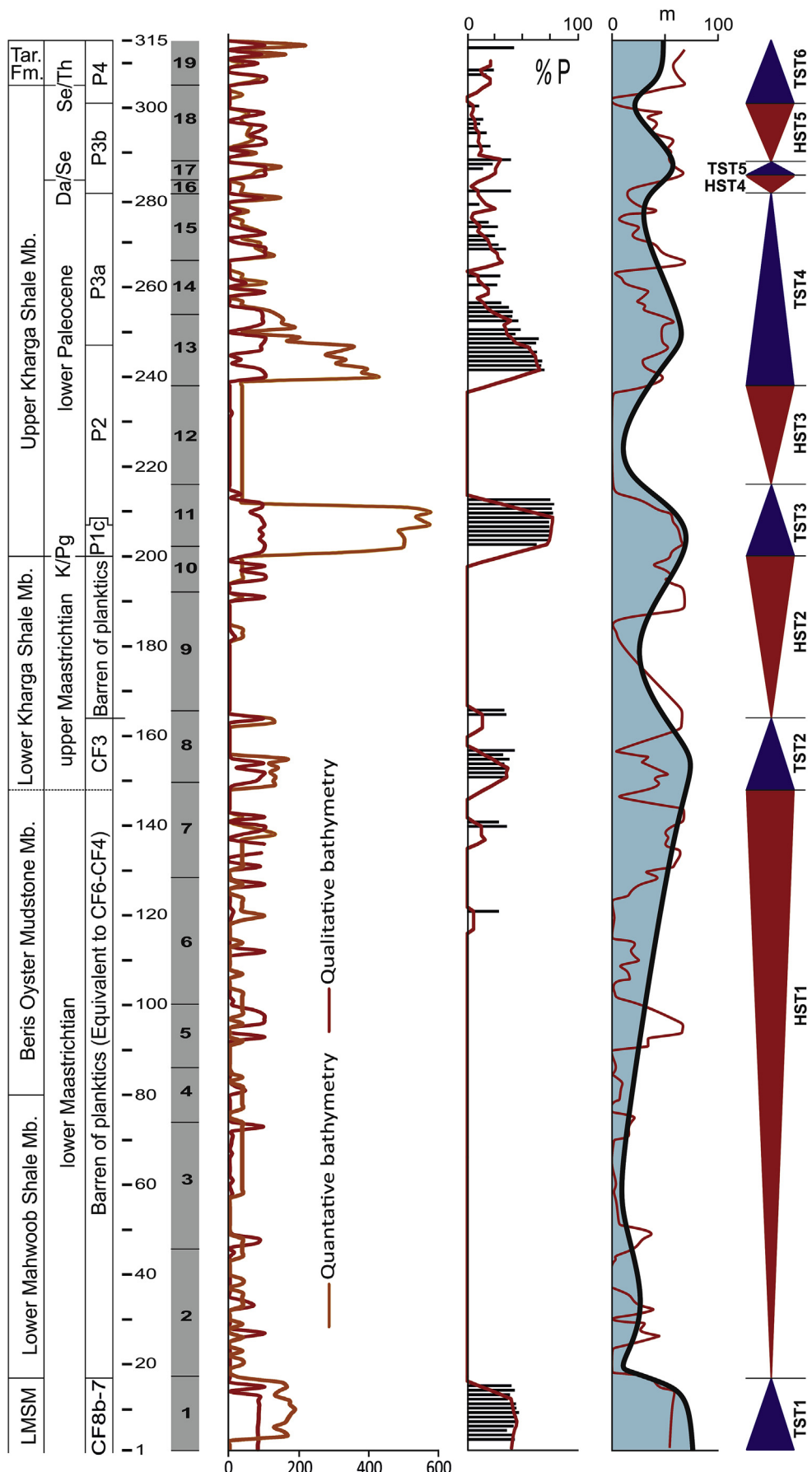


Fig. 7. Comparison of quantitative and qualitative sea level curves. The dark line (red) in %P is a 5-point running average. (For interpretation of the references to color in this figure legend, the reader is referred to the web version of this article.)

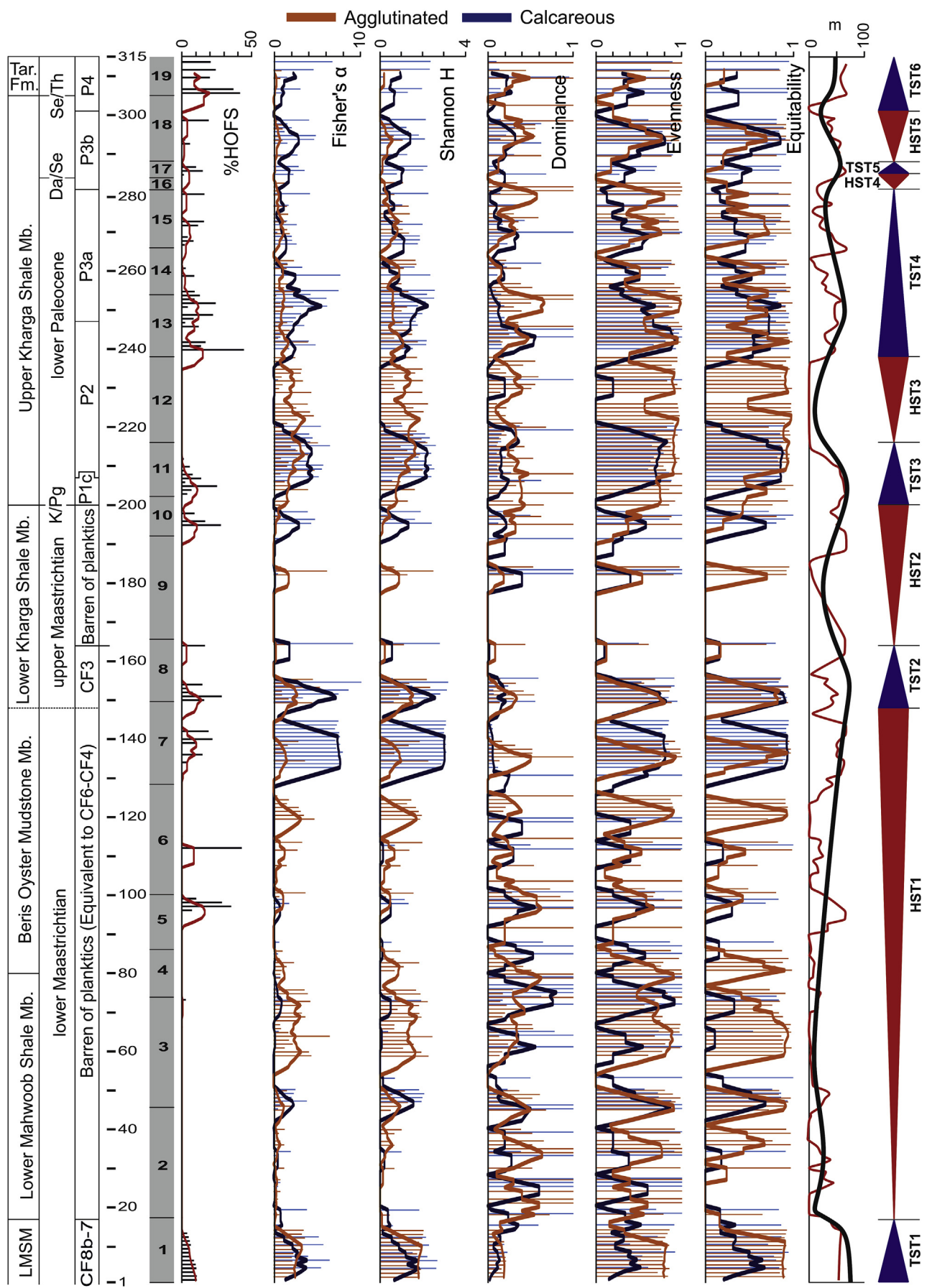


Fig. 8. Comparison of agglutinated and calcareous benthic foraminiferal diversity proxies. All dark lines (red) are 5-point running averages. (For interpretation of the references to color in this figure legend, the reader is referred to the web version of this article.)

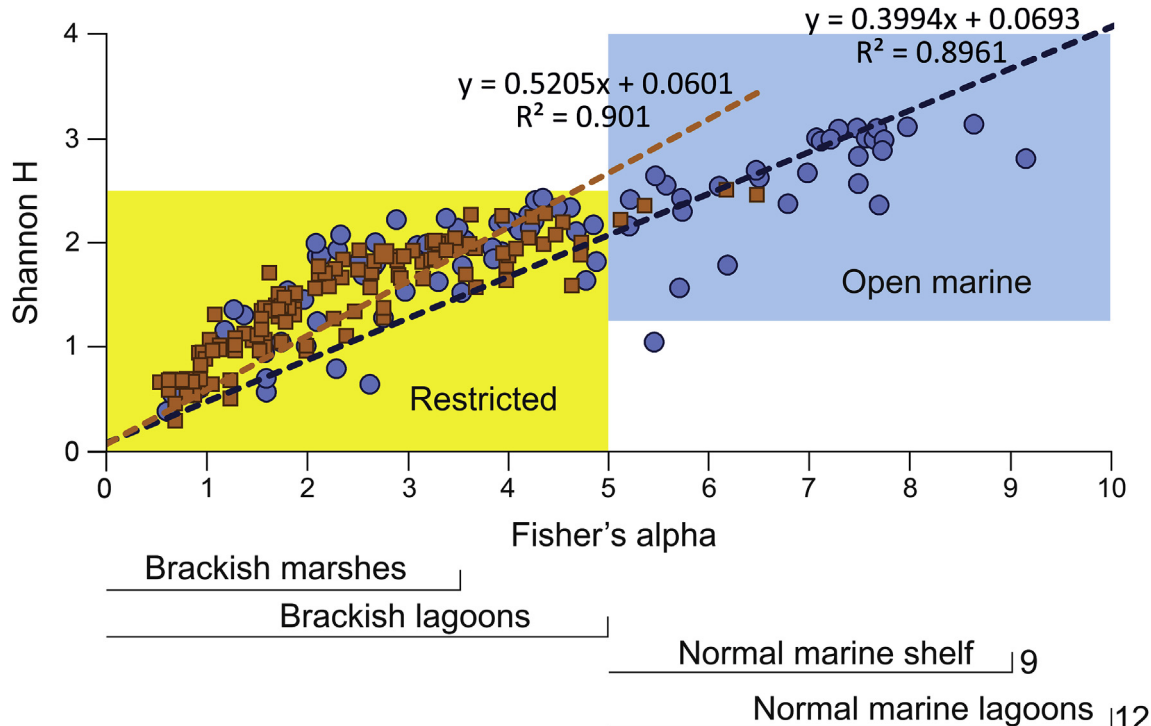


Fig. 9. Comparison of agglutinated and calcareous benthic foraminiferal community structure and depositional environment. Only four square agglutinated data points plot in the open marine region. They are: 1: sample 216 (TST3); 2: sample 153 (TST2); 3: sample 183 (HST2); 4: sample 63 (HST1). Samples 1, 2 and 3 belong to the deeper water agglutinated biofacies 3 (*Trochammina*) and sample 4 to the shallower biofacies 3 (see also Table 1).

Recently, from New Zealand, Hayward (2014) proposed a model while explaining the distribution of modern shallow water (<25 m) monospecific foraminiferal faunas from sheltered estuary, harbor, and lagoon with diversity values rarely exceeding 1. The present agglutinated foraminiferal dataset mirrors this distribution pattern (see Fig. 12), albeit with much higher species diversity and intermittent marine incursions, and hence, with a somewhat deeper depth, as also evidenced by the presence of planktic and characteristic benthic foraminifera species.

7.1. Comparative Low- and high-latitude fauna

It is tempting to compare shallow water agglutinated low- and high-latitude Cretaceous-Paleogene fauna. However, such studies for the latter are rare. Kaminski et al. (1988) did provide a comparative account of the low- (data from SE Trinidad) and high-latitude fauna [Polish Flysch Carpathians, Labrador and NE Newfoundland Margin, Central North Sea, Nungssuaq, West Greenland and Norwegian-Greenland Sea (DSDP Sites 345, 346, 347, 349 and 350)], based on the occurrences of 187 agglutinated species. Of these, only 8 are common (*Spiroplectinella dentata*, *Trochammina globigeriniformis*, *Ammodiscus cretaceus*, *Trochammina deformis*, *Haplophragmoides glabra*, *Cribrostomoides trinitatis*, *Gaudryina pyramidata* and *Clavulinoides trilaterus*; see Appendix 9); 6 with those occurring at NE Trinidad (of the eight, *T. globigeriniformis* and *T. deformis* are absent) and in the Maastrichtian to Paleogene formations of the Polish Flysch Carpathians (*Haplophragmoides glabra* being absent) and 5 each with the Maastrichtian to Eocene deposits in Labrador and NE Newfoundland Margin wells and the Danian to Eocene sedimentary rocks from Central North Sea wells (*C. trinitatis*, *G. pyramidata* and *C. trilaterus* are absent; see Appendix 9). There is little similarity with West Greenland and understandable with deeper DSDP

sites. Quite clearly, in spite of this meager data, species differentiation is pronounced, although genera differentiation is much reduced, suggesting the increased role of regional factors such as the availability of food, ventilation of bottom waters and regional tectonics. Biofacial comparisons, although desirable, is not possible, for now.

8. Conclusions

The shallow water (<100 m) Maastrichtian–Thanetian agglutinated foraminifera suggest an equitable benthic environment deposited in a brackish littoral and/or marsh setting. Five agglutinated biofacies are recognized that reflect not only the prevailing paleoenvironment but also the paleodepth. Statistical analysis bears out that both *Haplophragmoides* and *Ammobaculites* show a preference for shallower depths, however, *Trochammina* prefers deeper. The distribution of other dominant agglutinated genera *Gaudryina*, *Ammomarginulina*, *Spiroplectinella* and *Cribrostomoides* are positively and significant correlated with paleodepth. Sea level curves using characteristic benthic foraminiferal species, genera and assemblages corroborate the quantitatively generated estimate and statistical analysis. Data suggests that in the absence of or of an impoverished benthic foraminiferal fauna, a high resolution agglutinated foraminiferal dataset can be good predictor of the benthic community structure and environment, similar to the results arrived at from its calcareous counterpart, at least for shallow settings (<100 m). Faunal changes at boundaries (Cretaceous–Paleogene, Danian–Selandian and Selandian–Thanetian) are evaluated; the change before and after the K–Pg is most dramatic; the fauna changes from a *Trochammina*-dominated to a *Haplophragmoides*-dominated environment, from an epifaunal to a shallow infaunal habitat, from eutrophic to a mesotrophic environment, suggesting an increased role of organic flux.

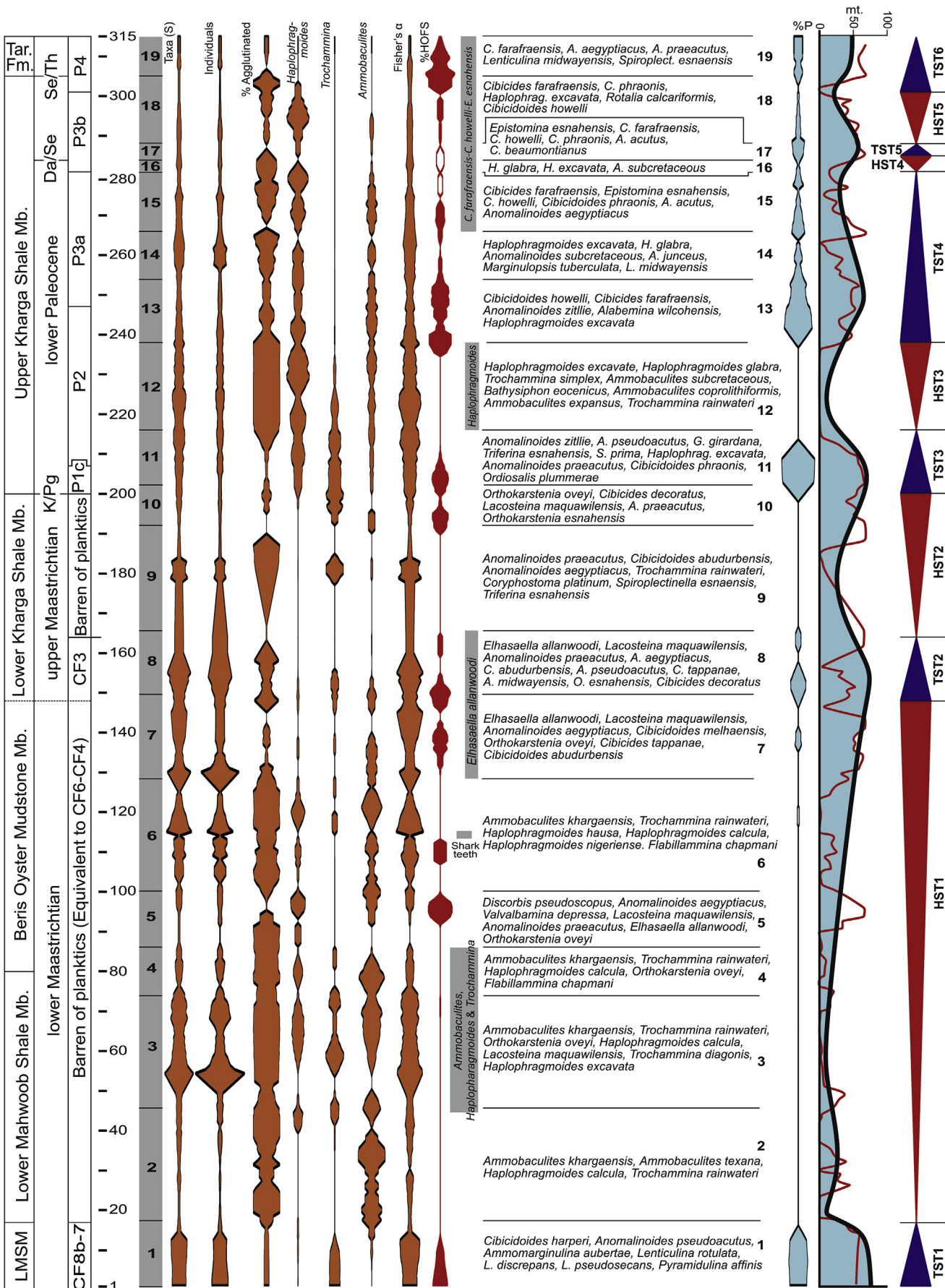


Fig. 10. Summary of events for the studied section.

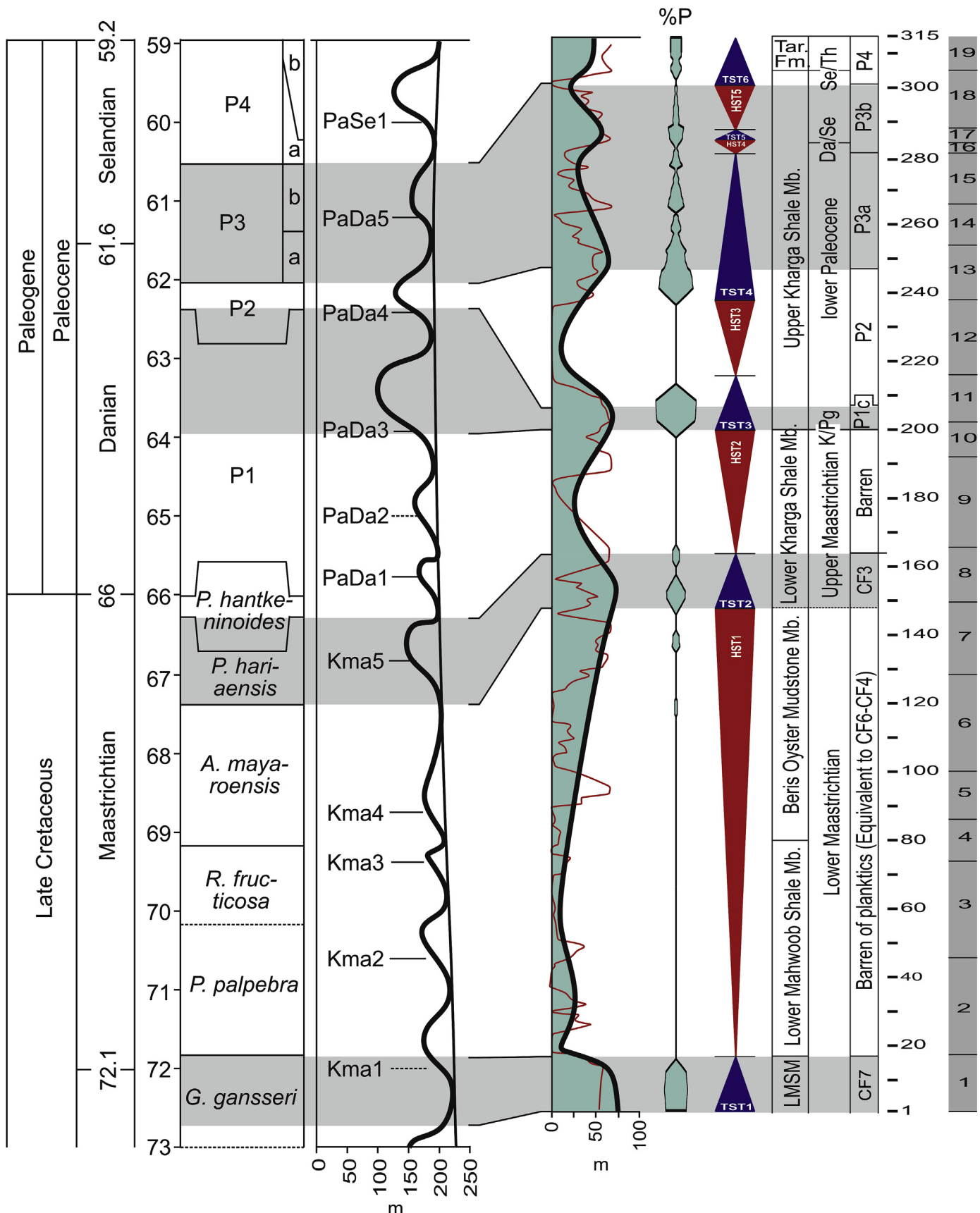


Fig. 11. Correlation of the sea level curve of Haq (2014) with the present inferred sea level curve.

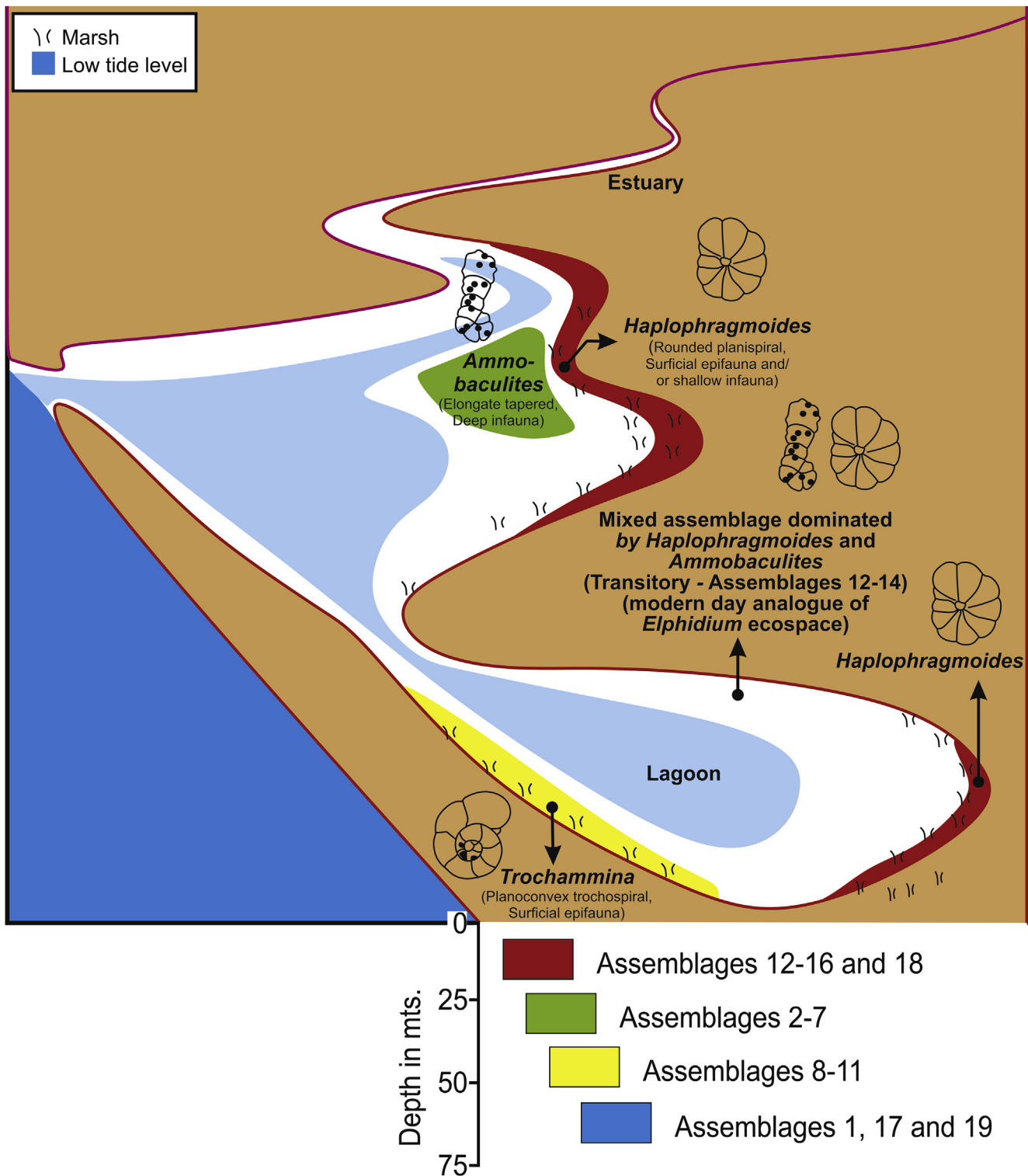


Fig. 12. Possible special distribution of the three most dominant genera (and biofacies) encountered in the present study along with possible position of the inferred 19 benthic foraminiferal assemblages (see Table 1 for assemblage numbers).

Acknowledgements

SJ acknowledges office space from Head of Department of Geology, Adama Science and Technology University, Adama (Ethiopia). The study was improved following suggestions by two anonymous reviewers and the editor Dr. Eduardo A. M. Koutsoukos.

References

- Abd El Hameed, A.T., 1973. Micropaleontological studies on some Upper Cretaceous agglutinated foraminifera from Egypt. Unpublished M.Sc. Thesis, Assiut University, 139 pp.
- Awad, G.H., Ghobrial, M.G., 1965. Zonal stratigraphy of the Kharga Oasis. Geological Survey of Egypt, Cairo, Paper No. 34, 77 pp.

- Barthel, K.W., Herrmann-Degen, W., 1981. Late Cretaceous and Early Tertiary stratigraphy in the Great Sand Sea and its SE Margins (Farafra and Dakhla Oases), SW Desert, Egypt. *Mitteilungen der Bayerischen Staatssammlung für Paläontologie und Historische Geologie* 21, 141–182.
- Berggren, W.A., 1974a. Late Paleocene–early Eocene benthonic foraminiferal biostratigraphy and paleoecology of Rockall bank. *Micropaleontology* 20, 426–448.
- Berggren, W.A., 1974b. Paleocene benthonic foraminiferal biostratigraphy, biogeography, and paleoecology of Libya and Mali. *Micropaleontology* 20, 449–465.
- Berggren, W.A., Pearson, P.N., 2005. A revised tropical to subtropical Paleogene planktonic foraminiferal zonation. *Journal of Foraminiferal Research* 35, 279–298.
- El-Azabi, M.H., Farouk, S., 2011. High-resolution sequence stratigraphy of the Maastrichtian–Ypresian succession along the eastern scarp face of Kharga Oasis, southern Western Desert, Egypt. *Sedimentology* 58, 579–617.
- El Nady, M.M., Hammad, M.M., 2015. Organic richness, kerogen types and maturity in the shales of the Dakhla and Duwi formations in Abu Tartur area, Western Desert, Egypt: implication of Rock–Eval pyrolysis. *Egyptian Journal of Petroleum* 24, 423–428.
- Faris, M., 1974. Geological and paleontological studies on the Late Cretaceous–Early Tertiary succession in Qena region and Kharga Oasis. M. Sc. Thesis, Assiut Univ., 189 pp.
- Faris, M., Farouk, S., 2012. Integrated biostratigraphy of the Upper Maastrichtian–Paleocene successions in north-central Sinai, Egypt. *Geologia Croatica* 65, 139–160.
- Farouk, S., 2014. Maastrichtian carbon cycle changes and planktonic foraminiferal bioevents at Gebel Matulla, west-central Sinai, Egypt. *Cretaceous Research* 50, 238–251.
- Farouk, S., 2016. Paleocene stratigraphy in Egypt. *Journal of African Earth Sciences* 113, 126–152.
- Farouk, S., El-Sorogy, E., 2015. Danian/Selandian unconformity in the central and southern Western Desert of Egypt. *Journal of African Earth Sciences* 103, 42–53.
- Farouk, S., Jain, S., 2016. Benthic foraminiferal response to relative sea-level changes in the Maastrichtian–Danian succession at the Dakhla Oasis, Western Desert, Egypt. *Geological Magazine* 2016, 1–18. <http://dx.doi.org/10.1017/S0016756816001023>.
- Galeotti, S., Kaminski, M.A., Coccioni, R., Speijer, R.P., 2004. High-resolution deep-water agglutinated foraminiferal record across the Paleocene/Eocene transition in the Contessa Road Section (central Italy). In: Bubík, M., Kaminski, M.A. (Eds.), *Proceedings of the Sixth International Workshop on Agglutinated Foraminifera*, vol. 8. Grzybowski Foundation Special Publication, pp. 83–103.
- Gebhardt, B., 1998. Benthic foraminifera from the Maastrichtian Lower Mamu Formation near Leri (Southern Nigeria): paleoecology and paleogeographic significance. *Journal of Foraminiferal Research* 28, 76–89.
- Haq, B.U., 2014. Cretaceous eustasy revisited. *Global and Planetary Change* 113, 44–58.
- Hayward, B.W., 2014. “Monospecific” and Near–Monospecific benthic foraminiferal faunas, New Zealand. *Journal of Foraminiferal Research* 44, 300–315.
- Hewaidy, A.A., El-Azabi, M.H., Farouk, S., 2006. Facies associations and sequence stratigraphy of the Upper Cretaceous–Lower Eocene succession in the Farafra Oasis, Western Desert, Egypt. 8th International Conference on the Geology of the Arab World (GAW 8), Cairo University, Egypt 2 569–599.
- Hewaidy, A.G., Farouk, S., Hatem, A., Bazeen, Y., 2014. Maastrichtian to Paleocene agglutinated foraminifera from the Dakhla Oasis, Western Desert, Egypt. *Egyptian Journal of Paleontology* 14, 1–38.
- van Hinsbergen, D.J.J., Kouwenhoven, T.J., van der Zwaan, G.J., 2005. Paleobathymetry in the backstripping procedure: correction for oxygenation effects on depth estimates. *Palaeogeography, Palaeoclimatology, Palaeoecology* 221, 245–265.
- Huber, B.T., Macleod, K.G., Tur, N.A., 2008. Chronostratigraphic framework for upper Campanian–Maastrichtian sediments on the Blake nose (subtropical north Atlantic). *Journal of Foraminiferal Research* 38, 162–182.
- Issawi, B., 1972. Review of Upper Cretaceous–Lower Tertiary stratigraphy in central and southern Egypt. *American Association of Petroleum Geologists, Bulletin* 56, 1448–1473.
- Kaminski, M.A., 1987. Cenozoic Deep-Water Agglutinated Foraminifera in the North Atlantic. Unpublished Thesis. Woods Hole Oceanographic Institution, Woods Hole, MA, USA, 282 p.
- Kaminski, M.A., Geroch, S., 1992. The use of deep-water agglutinated Foraminifera in correlating Lower Cretaceous pelagic and flysch sequences: current status and prospects for the future. *Cretaceous Research* 13 (5–6), 453–466.
- Kaminski, M.A., Gradstein, F.M., Berggren, W.A., Geroch, S., Beckmann, J.P., 1988. Flysch-type agglutinated foraminiferal assemblages from Trinidad: taxonomy, stratigraphy and palaeobathymetry. In: *Proceedings of the Second Workshop on Agglutinated Foraminifera*. Vienna 1986. Abhandlungen der Geologischen Bundesanstalt, vol. 41, pp. 155–227.
- Kaminski, M.A., Setoyama, E., Cetean, C.G., 2008. Revised Stratigraphic Ranges and the Phanerozoic Diversity of Agglutinated Foraminiferal Genera. In: Kaminski, M.A., Coccioni, R. (Eds.), *Proceedings of the seventh international workshop on agglutinated foraminifera*, vol. 13. Grzybowski Foundation Special Publication, pp. 79–106.
- Kaminski, M.A., Setoyama, E., Cetean, C.G., 2010. The Phanerozoic diversity of agglutinated foraminifera: origination and extinction rates. *Acta Palaeontologica Polonica* 55, 529–539.
- Keller, G., Li, L., MacLeod, N., 1995. The Cretaceous/Tertiary boundary stratotype section at El Kef, Tunisia: how catastrophic was the mass extinction? *Palaeogeography, Palaeoclimatology, Palaeoecology* 119, 221–254.
- Keller, G., Adatte, T., Burns, S.J., Tantawy, A.A., 2002. High-stress paleoenvironment during the late Maastrichtian to early Paleocene in Central Egypt. *Palaeogeography, Palaeoclimatology, Palaeoecology* 187, 35–60.
- Kochhann, K.G.D., Koutsoukos, E.A.M., Gerson, F., 2014. Aptian-Albian benthic foraminifera from DSDP Site 364 (offshore Angola): a paleoenvironmental and paleobiogeographic appraisal. *Cretaceous Research* 48, 1–11.
- Koutsoukos, E.A.M., Hart, M.B., 1990. Cretaceous foraminiferal morphogroup distribution patterns, paleocommunities and trophic structures: a case study from the Sergipe Basin Brazil. *Transactions of the Royal Society of Edinburgh: Earth Sciences* 51, 221–246.
- Kuhnt, W., Urquhart, E., 2001. Tethyan flysch-type benthic foraminiferal assemblages in the North Atlantic: cretaceous to Palaeogene deep water agglutinated foraminifers from the Iberia abyssal plain (ODP Leg 173). *Revue de Micropaléontologie* 44 (1), 27–58.
- Kuhnt, W., Moullade, M., Kaminski, M.A., 1996. Ecological structuring and evolution of deep sea agglutinated foraminifera — a review. *Revue de Micropaléontologie* 39 (4), 271–281.
- Li, L., Keller, G., Stennesbeck, W., 1999. The Late Campanian and Maastrichtian in northwestern Tunisia: paleoenvironmental inferences from lithology, macrofauna and benthic foraminifera. *Cretaceous Research* 20, 231–252.
- Lüger, P., 1985. Stratigraphie der marinen Oberkreide und des Alttertiärs im südlichen Obernil–Becken (SW–Ägypten) unter besonderer Berücksichtigung der Mikropaläontologie, Palökologie und Paläogeographie. Berliner geowissenschaftliche Abhandlungen Reihe A 63, 1–151.
- Lüger, P., 1988a. Campanian to Paleocene Agglutinated Foraminifera from Freshwater Influenced Marginal Marine (Deltaic) Sediments of Southern Egypt, vol. 41. Abh. Geol. B.-A., pp. 255–263.
- Lüger, P., 1988b. Maastrichtian to Paleocene facies evolution and Cretaceous/Tertiary boundary in middle and southern Egypt. *Revista Española de Micropaleontología*, Numero Extraordinario 83–90.
- Nagy, J., Kaminski, M.A., Kuhnt, W., Bremer, M.A., 2000. Agglutinated foraminifera from neritic to bathyal facies in the Palaeogene of Spitsbergen and the Barents Sea. In: Hart, M.B., Kaminski, M.A., Smart, C.W. (Eds.), *Proceedings of the Fourth International Workshop on Agglutinated Foraminifera*, vol. 7. Grzybowski Foundation Special Publication, pp. 333–361.
- Nagy, J., Jargvoll, D., Dypvik, H., Jochmann, M., Riber, L., 2013. Environmental changes during the paleocene-eocene thermal maximum in spitsbergen as reflected by benthic foraminifera. *Polar Research* 32, 19737. <http://dx.doi.org/10.3402/polar.v32i0.19737>.
- Obaidalla, N.A., El-Dawy, M.H., Kassab, A.S., 2009. Biostratigraphy and paleoenvironment of the Danian/Selandian (D/S) transition in the Southern Tethys: a case study from north Eastern Desert, Egypt. *Journal of African Earth Science* 53, 1–15.
- Olsson, R.K., Nyong, E.F., 1984. A paleosecope model for Campanian lower Maastrichtian foraminifera of New Jersey and Delaware. *Journal of Foraminiferal Research* 14, 50–68.
- Orabi, H.O., 1995. Biostratigraphy and paleoecology of the Campanian–Paleocene agglutinated foraminifera from Gebel Um El Ghanayim, Kharga Oasis, Egypt. *Science Journal. Faculty of Science, Menoufia University* 11, 25–68.
- Orabi, H.O., 2000. Foraminiferal morphogroups and paleoenvironments of some Upper Cretaceous exposures in Egypt. *Egyptian Journal of Geology* 44, 359–397.
- Petters, S.W., 1979. Paralic arenaceous foraminifera from the upper cretaceous of the Benue Trough, Nigeria. *Acta Palaeontologica Polonica* 24, 451–471.
- Said, R., 1962. *The Geology of Egypt*. Elsevier, 377 pp.
- Setoyama, E., Kaminski, M.A., Tyszka, J., 2011. The Late Cretaceous–Early Paleocene paleobathymetric trends in the southwestern Barents Sea — paleoenvironmental implications of benthic foraminiferal assemblage analysis. *Palaeogeography, Palaeoclimatology, Palaeoecology* 307 (1–4), 44–58.
- Speijer, R.P., 1994. Extinction and recovery patterns in benthic foraminiferal paleocommunities across the Cretaceous/Paleogene and Paleocene/Eocene boundaries. *Geologica Ultrajectina* 124, 191 pp.
- Speijer, R.P., 2003. Danian–Selandian sea-level change and biotic excursion on the southern Tethyan margin (Egypt). In: Wing, S.L., Gingerich, P.D., Schmitz, B., Thomas, E. (Eds.), *Causes and Consequences of Globally Warm Climates in the Early Paleogene*. Geological Society of America Special Paper 369, pp. 275–290.
- Sprong, J., Kouwenhoven, T.J., Bornemann, A., Schulte, P., Steurbaut, E., Youssef, M., Speijer, R.P., 2012. Characterization of the Latest Danian Event by means of benthic foraminiferal assemblages along a depth transect at the southern Tethyan margin (Nile Basin, Egypt). *Marine Micropaleontology* 86–87, 15–31.
- Tantawy, A.A., Keller, G., Adatte, T., Stennesbeck, W., Kassab, A., Schulte, P., 2001. Maastrichtian to Paleocene depositional environment of the Dakhla Formation, Western Desert, Egypt: sedimentology, mineralogy, and integrated micro- and macrofossil biostratigraphies. *Cretaceous Research* 22, 795–827.
- Van Der Zwaan, G.J., Duijnstee, I.A.P., Den Dulk, M., Ernst, S.R., Jannink, N.T., Kouwenhoven, T.J., 1999. Benthic foraminifers: proxies or problems? A review of paleoecological concepts. *Earth Science Reviews* 46, 213–236.
- Wade, B.S., Pearson, P.N., Berggren, W.A., Pálike, H., 2011. Review and revision of Cenozoic tropical planktonic foraminiferal biostratigraphy and calibration to the geomagnetic polarity and astronomical time scale. *Earth-Science Reviews* 104, 111–142.

Appendix A. Supplementary data

Supplementary data related to this article can be found at <http://dx.doi.org/10.1016/j.cretres.2017.06.012>.